



**Forest damage inventory using the local pivotal sampling method**

Journal:	<i>Canadian Journal of Forest Research</i>
Manuscript ID	cjfr-2016-0411.R1
Manuscript Type:	Article
Date Submitted by the Author:	05-Dec-2016
Complete List of Authors:	Roberge, Cornelia; Sveriges Lantbruksuniversitet Fakulteten for Skogsvetenskap, Forest resource management Grafström, Anton; Swedish University of Agricultural Sciences, Department of Forest Resource Management Ståhl, Göran; Swedish University of Agricultural Sciences, Forest Resource Management
Keyword:	Forest damage inventory, Forest health, Local pivotal method, Two-phase sampling for stratification, Double sampling

SCHOLARONE™  
Manuscripts

## 1 **Forest damage inventory using the local pivotal sampling method**

2 Cornelia Roberge, Anton Grafström and Göran Ståhl

3 Cornelia Roberge

4 Department of Forest Resource Management,

5 Swedish University of Agricultural Sciences (SLU),

6 901 83 Umeå, Sweden.

7 Fax: +46 (0)90 778 116

8 Tel: +46 (0)90 786 83 70

9 e-mail: [cornelia.roberge@slu.se](mailto:cornelia.roberge@slu.se)

10 Anton Grafström

11 Department of Forest Resource Management,

12 Swedish University of Agricultural Sciences (SLU),

13 901 83 Umeå, Sweden.

14 e-mail: [anton.grafstrom@slu.se](mailto:anton.grafstrom@slu.se)

15 Göran Ståhl

16 Department of Forest Resource Management,

17 Swedish University of Agricultural Sciences (SLU),

18 901 83 Umeå, Sweden.

19 e-mail: [goran.stahl@slu.se](mailto:goran.stahl@slu.se)

20

Draft

## 21 Abstract

22 Specially designed forest damage inventories, directed to areas with potential or suspected damage, are  
23 performed in many countries. In this study we evaluate a new approach for damage inventories where  
24 auxiliary data are used for the sample selection with the recently introduced local pivotal sampling  
25 design. With this design, a sample that is well spread in the space of the auxiliary variables is obtained.  
26 We applied Monte Carlo sampling simulation to evaluate whether this sampling design leads to more  
27 precise estimates compared to commonly applied baseline methods. The evaluations were performed  
28 using different damage scenarios and different simulated relationships between the auxiliary data and  
29 the actual damages. The local pivotal method was found to be more efficient than simple random  
30 sampling in all scenarios and, depending on the allocation of the sample and the properties of the  
31 auxiliary data, it sometimes outperformed two-phase sampling for stratification. Thus, the local pivotal  
32 method may be a valuable tool to cost-efficiently assess the magnitude of forest damage once  
33 outbreaks have been detected in a forest region.

34  
35 Keywords: Forest damage inventory, Forest health, Local pivotal method, Two-phase sampling for  
36 stratification, double sampling

## 38 Résumé

39  
40 Dans plusieurs pays, des inventaires de dommages forestiers spécialement conçus sont utilisés dans des  
41 régions avec dommages potentiels ou soupçonnés. Dans la présente étude, nous évaluons une nouvelle  
42 approche pour les inventaires de dommages forestiers où des données auxiliaires sont utilisées pour la  
43 sélection de l'échantillon en utilisant la méthode du pivot local d'échantillonnage. Cette approche  
44 permet d'obtenir un échantillon qui est bien réparti dans l'espace des variables auxiliaires. Nous avons

45 utilisé des simulations Monte Carlo pour évaluer si cette méthode donne des estimés plus précis  
46 comparativement à d'autres méthodes communes. Les évaluations ont été faites en utilisant différents  
47 scénarios de dommage et différentes relations simulées entre les données auxiliaires et le dommage  
48 réel. La méthode du pivot local s'est avéré plus efficace que l'échantillonnage aléatoire simple pour tous  
49 les scénarios et, dépendant de la répartition de l'échantillon et des propriétés des données auxiliaires,  
50 elle surpassait parfois l'échantillonnage à deux phases pour stratification. En somme, la méthode du  
51 pivot local peut être un outil de choix pour l'évaluation efficace de l'amplitude des dommages forestiers  
52 lorsque des épidémies ont été détectées dans une région donnée.

53

## 54 **Introduction**

55 The world's forests provide numerous ecosystem services (e.g. Mery et al. 2005). However, concerns  
56 have been raised that the world's forests are under increasing stress due to global change (Trumbore, et  
57 al. 2015). One example is stress to forest trees due to heat and drought (Allen, et al. 2010) which may  
58 increase forest damage (Dale et al. 2001), thereby potentially limiting the forests' capacity to provide  
59 ecosystem services (Mery et al. 2005). As part of responsible forest management, many countries have  
60 developed forest health monitoring schemes for identifying and investigating potential threats to the  
61 forest resource, e.g. USA (Bennett and Tkaz 2008), Australia (Carnegie 2008), Sweden (Wulff et al. 2012)  
62 and Norway (Aamlid et al. 2000). In many cases the schemes include some form of aerial detection  
63 survey or sketch-mapping (e.g. Backsen and Howell, 2013), and the usefulness of remotely sensed data  
64 is increasingly acknowledged (Hall et al. 2016). In addition to detecting the presence of damage, there is  
65 often a need to identify the damaging agent and to accurately quantify the extent of damage for  
66 informed decisions (Wulff et al., 2012). This usually requires data obtained from field inventories,  
67 whether it is used for training or validating a model to map the extent of damage, or for producing a  
68 statistical estimate (e.g. the number of damage trees, or affected volume/area). It is important to have

69 reliable information for which the uncertainty can be specified. Therefore, estimates based on design-  
70 based inference are often required (Ferretti, 2009). In a study by Roberge et al (2016) it was found that  
71 great gains in precision can be obtained with two-stage-sampling for stratification, using existing  
72 national forest inventory plots as a first phase. Moreover, using forest damage maps for post-  
73 stratification improved the precision further.

74  
75 There is ongoing work in the field of mathematical statistics where new sampling methods that utilize  
76 auxiliary variables for selecting samples are being developed. A sample that is well spread, i.e. balanced  
77 in the auxiliary space, provides a good representation of the sampled population (Grafström and Schelin  
78 2013, Grafström and Lundström 2013) and thus results in precise estimates of the target parameter in  
79 case there is a strong relationship between the target variable and the auxiliary variables. The local  
80 pivotal method (LPM) was introduced by Grafström et al. (2012). The LPM utilizes distance in the  
81 auxiliary space to identify similar units that compete for inclusion in the sample. In that way the LPM  
82 avoids selection of nearby units and forces the sample to become well spread. It has recently been  
83 evaluated in the estimation of forest variables such as basal area, standing volume and mean height  
84 (Grafström and Ringvall, 2013, Grafström et al. 2014). The LPM method of sample selection is now  
85 available in the R (R Core Team 2016) package `BalancedSampling` (Grafström and Lisic, 2016).

86 The aim of this study was to provide a first test of LPM in the context of forest damage inventory. For  
87 comparison, two well-known baseline methods were also evaluated: simple random sampling (SI) and  
88 two-phase sampling for stratification (2PS) with a systematic random sample (SYS) in the first phase and  
89 stratified random sampling (STSI) in the second phase. Here, two strata were used for the STSI: grid-cells  
90 classified as damaged or undamaged. With the LPM method, the samples were spread geographically  
91 and in the space of auxiliary data. The efficiencies of the three different sampling strategies were  
92 compared through Monte Carlo simulation, using simulated forest damage populations of spruce bark

93 beetle (*Ips typographus*) and simulated auxiliary data in the form of damage tree counts, mimicking  
94 auxiliary data that could be obtained from, e.g., interpretation of aerial photos or a systematic  
95 helicopter inventory of each grid-cell in an area of interest. Remotely sensed data for directing the  
96 sample selection might also be obtained from other sources; such as digital color-infrared aerial  
97 photographs (Murtha and Wiart 2010), high resolution satellite imagery (Hais et al. 2009), satellite radar  
98 (Ortiz et al. 2013), airborne laser scanner data (Solberg 2010) or hyperspectral imaging (Näsi et al. 2015).  
99 For good back-ground and reviews of remote sensing of forest damage we refer to Hall et al. (2016),  
100 Rullan-Silva et al. (2013) and Ciesla (2000).

## 101 **Materials and Methods**

102 The different sampling strategies were applied for estimating the number of damage trees in four  
103 different simulated populations of bark beetle damage. We used a quadrat-shaped area of interest (AOI)  
104 located in the Swedish county of Västernorrland (cf. Roberge et al. 2016) to represent a typical  
105 municipality of 900 km<sup>2</sup>, divided into 1,200 × 1,200 grid-cells of 25 × 25 meters each. The AOI had a  
106 forest cover of 80% and comprised 13,870 forest stands in the segmented kNN-Sweden data (Reese et  
107 al. 2003) used for simulating the damage populations (Figure 1, Table 1). The auxiliary data used for the  
108 sample selection were the spatial coordinates (XY) of the grid-cells, damage tree counts (DTC, i.e.  
109 numbers of detected damage trees in grid-cells), and grid-cells classified as containing damage trees (D)  
110 or not (a binary variable). The 2PS and LPM designs start with a first-phase large systematic sample for  
111 which XY, DTC, and D auxiliary data were made available (the first phase sample sizes are 10,000 and  
112 3,600). Second phase samples were drawn (with sample sizes 50, 100, 150 and 200), using either LPM or  
113 STSI, from this systematic sample.

114 SI does not use any of the auxiliary information and the sample is selected entirely at random from the  
115 population of grid-cells. For the 2PS design we used the D auxiliary data for partitioning the first-phase

116 sample selected from the AOI into two strata. In each stratum, SI sampling was applied. LPM was used  
117 with equal probabilities, including grid-cells where no damage was detected (DTC=0).

### 118 **Inventory strategies**

119 The true number of damage trees in the AOI is the sum of damage trees over all grid-cells in the area:

$$120 \quad (1) \quad Y = \sum_{i=1}^N y_i$$

121 where  $N$  is the total number of grid-cells in the AOI and  $y_i$  is the number of damage trees in grid-cell  $i$ .

122 The baseline inventory methods are two commonly used sampling designs: SI from the whole AOI, and  
123 2PS, which utilizes the auxiliary information in sample selection. The two baseline methods were  
124 compared with LPM, which uses multiple auxiliary data sources for the sample selection. 2PS has been  
125 frequently applied in forest damage inventories over the years (Lucas 2009, Roberge et al. 2016). Both  
126 LPM and 2PS were based on an initial systematic sample of  $n_1$  grid-cells spread in geographical (XY)  
127 space. For the grid-cells sampled in the first phase, auxiliary data (XY, DTC and D) were made available.  
128 From the first-phase sample a second-phase sample was selected using LPM or STSI designs. The LPM  
129 spread the second phase sample in the XY and DTC auxiliary data spaces with equal inclusion  
130 probabilities (in this application). The 2PS design used the D auxiliary space to apply STSI sampling in the  
131 second phase, with predetermined sample sizes. In STSI, 20 or 40% of the sample was allocated to the  
132 strata without detected damage and the rest of the sample to the stratum where  $DTC \geq 1$  (i.e.  $D=1$ ). The  
133 two different allocation principles were selected in order to assess whether a larger or a smaller  
134 proportion of the sample should be selected in the stratum without detected damage, although in both  
135 cases the majority of the plots were allocated to the stratum with detected damage. This led to two sets  
136 of results for the 2PS design denoted '2PS\_20' (20%) and '2PS\_40' (40%). For both 2PS and LPM we  
137 investigated the impacts of different errors in the auxiliary data, in the form of errors of omission and  
138 commission of different sizes.

139 **Estimators**

140 We used the  $\pi^*$ -estimator (Särndal et al. 1992, p. 348) where each included grid-cell value is divided by  
 141 its inclusion probability. This results in the regular HT-estimator for the population total, for LPM:

$$142 \quad (2) \quad \hat{Y}_{LPM} = \frac{N}{n_1} \frac{n_1}{n} \sum_{i=1}^n y_i = N \bar{y}_s$$

143 where  $N$  is all grid-cells,  $n_1$  is the first-phase sample size and  $n$  is the sample size selected in the second  
 144 phase. The mean,  $\bar{y}_s$  is the sample mean from the second phase (S2) sample. For the 2PS design (Särndal  
 145 et al. 1992, p. 353) we used the following estimator for the population total

$$146 \quad (3) \quad \hat{Y}_{2PS} = N \sum_{h=1}^{H_{S1}} w_{ah} \bar{y}_{sh} = N \hat{y}_U$$

147 where  $w_{ah} = n_{1,h}/n_1$  (i.e. the relative size of stratum  $h$  in the first phase sample), and  $\bar{y}_{sh}$  the mean of  
 148 the value of interest within stratum  $h$ . In this application only two strata were used ( $H_{S1}=2$ ). The  
 149 estimated mean over all grid-cells ( $U$ ) in the AOI is denoted  $\hat{y}_U$ .

150 For the SI design the following estimator for the population total was used

$$151 \quad (4) \quad \hat{Y}_{SI} = \frac{N}{n} \sum_{i=1}^n y_i = N \bar{y}_s$$

152 **Variance estimation**

153 The variance of samples that are well-spread in auxiliary space can be estimated by applying the  
 154 following estimator:

$$155 \quad (5) \quad \hat{V}_{GS}(\hat{Y}_{LPM}) = \frac{1}{2} \sum_{i \in S} \left( \frac{y_i}{\pi_i} - \frac{y_{j_i}}{\pi_{j_i}} \right)^2$$

156 where  $j_i$  is the nearest neighbor to  $i$  in the realized sample, i.e. the nearest neighbor in terms of the  
 157 auxiliary space in which the sample is balanced (see Grafström and Schelin 2013). In addition a variance

158 estimator by Deville (1993), which also estimates the variance of an estimator without second order  
 159 inclusion probabilities, was applied:

$$160 \quad (6) \quad \hat{V}_D(\hat{Y}_{LPM}) = \frac{1}{1 - \sum_{i \in s} a_i^2} \sum_{i \in s} (1 - \pi_i) \left( \frac{y_i}{\pi_i} - \sum_{j \in s} a_j \frac{y_j}{\pi_j} \right)^2$$

161 Where  $a_i = (1 - \pi_i) / \sum_{j \in s} (1 - \pi_j)$  and  $s$  refers to the selected sample. For variance estimation of the  
 162 baseline designs (SI and 2PS) we refer to standard estimators provided in textbooks (e.g., Särndal et al.  
 163 1992, p. 353 for 2PS and p. 68 for SI).

### 164 **Simulated damage populations**

165 Damage populations were simulated with different spatial patterns and damage intensities to resemble  
 166 damage caused by the spruce bark beetle (*Ips typographus*) at different intensities. The forest landscape  
 167 was simulated using kNN-Sweden (Reese et al. 2003). First, two populations were simulated: one where  
 168 damage incidence is highly dependent on spruce volume (IPS), and another where this dependence is  
 169 less strong and the incidence of damage is less frequent (IPSALT). Details of these populations are  
 170 described in Table 1 and Roberge et al. (2016). Two additional populations were introduced to cover  
 171 important cases with a spatial trend in the number of damaged trees in affected pixels, with lower  
 172 intensities of damage trees towards the edges of the municipality for IPSS and IPSALTS. These new  
 173 damage populations were based on new realizations of IPS and IPSALT. Using the following functions,  
 174 the frequency of damage trees was made more concentrated in the center of a chosen epicenter and  
 175 decrease away from it:

$$176 \quad (7) \quad f(x, y) = g(x) * g(y)$$

177 Where  $x$  and  $y$  are the center coordinate of each grid-cell, and

$$178 \quad (7a) \quad g(x) = 1 - \left( \frac{|x - wx|}{lx} \right)$$

179 where  $wx$  was set to 1600000, a coordinate within the AOI, and  $lx = x_{max} - x_{min}$

180 (7b) 
$$g(y) = 1 - \left( \frac{|y - wy|}{2ly} \right)$$

181 where  $wy$  was set to 7035000, a chosen coordinate within the AOI and  $ly = y_{max} - y_{min}$ .

182 Eq. 7 returns values between 0.29 and 1 for each grid-cell (i.e. for each grid-cell coordinate  $x$  and  $y$ )  
 183 creating a diamond shaped area with the highest numbers close to the chosen center coordinates. The  
 184 values from this raster layer were multiplied with the realized numbers of damaged trees in the baseline  
 185 scenarios described by IPS and IPSALT (Roberge et al. 2016). The results (in terms of number of damage  
 186 trees) were rounded upwards. The resulting damage layer has higher damage tree counts near the  
 187 epicenter ( $wx, wy$ ).

### 188 Simulated auxiliary data

189 DTC data layers were simulated with different errors. They had detection and false-detection  
 190 probabilities equal for the whole municipality as described in Roberge et al. (2016) for the IPS scenarios.  
 191 These data layers correspond to classified remote sensing (RS) data, or the results of photo  
 192 interpretation or helicopter inventory. In this study, however, we used only the data available for the  
 193 first-phase grid-cells. The different combinations of detection probabilities and commission errors were  
 194 named with a number corresponding to the detection probability (90%, etc.) and a suffix providing the  
 195 level of commission error (L for 0.001 and H for 0.05). Hence, DTC90L and DTC90H refer to 90 %  
 196 detection and the lowest and highest probabilities of commission error, respectively.

### 197 Monte Carlo Simulations

198 For comparing the sampling strategies, Monte Carlo simulation was applied in the AOI for the different  
 199 populations. All estimators that we used are unbiased for the population totals (Table 1) and thus the  
 200 mean of estimated values approaches the true totals as the number of repetitions increases. The  
 201 empirical relative standard deviation (ERSD) of the estimators was calculated as:

202 (8) 
$$ERSD(\hat{Y}) = \frac{\sqrt{\frac{1}{M} \sum_{m=1}^M (\hat{Y}_m - Y)^2}}{Y}$$

203 Where  $Y$  is the true population total and  $\hat{Y}_m$  is the estimated value from the  $m$ :th repetition of the  $M$   
204 repetitions. In order to evaluate the variance estimators we also calculated the ratio ( $R$ ) of the empirical  
205 mean of each variance estimator to the empirical variance of the estimator:

206 (9) 
$$R = \frac{\frac{1}{M} \sum_{m=1}^M \hat{V}(\hat{Y}_{LPM})_m}{\frac{1}{M} \sum_{m=1}^M (\hat{Y}_m - Y)^2}$$

207 Simulations, analysis and visualizations were made with R (R Development Core Team 2016), using the R  
208 packages raster (Hijmans 2014), rgdal (Bivand et al. 2014), rasterVis (Perpinan Lamiguero and Hijmans  
209 2014), data.table (Dowle et al. 2014), ggplot2 (Wickham 2009), sampling (Tillé and Matei 2014) and  
210 BalancedSampling (Grafström and Lisic 2016).

## 211 Results

212 LPM resulted in a more even ERSD (across the different populations, auxiliary data, and sample sizes)  
213 compared to the 2PS design, and the ERSD for LPM was consistently lower than the ERSD for the SI  
214 design (figure 2 and 3, table 2). For good auxiliary data with appropriate allocation, the 2PS design  
215 resulted in the lowest ERSD.

216 ERSD from SI sampling in IPS was close to the ERSD from SI sampling in IPSS. Only at small sample sizes  
217 did the slightly smaller population variance of the IPSS lead to a slight difference in the ERSD when the  
218 two were compared for SI design. The other “twin” populations (IPSALT and IPSALTS) were also similar in  
219 ERSD and followed a similar pattern.

220 LPM applied to the two populations with most damage (IPS and IPSS) also resulted in similar ERSD, i.e.  
221 the ERSD from LPM sampling in IPS only differed slightly from the ERSD from LPM sampling in IPSS, with  
222 the same sample size and auxiliary data. LPM and the best auxiliary data scenario resulted in lower ERSD  
223 from sampling the IPSS population relative to the IPS population with the same estimator and auxiliary  
224 data for all sample sizes. The same pattern was found for the LPM design in IPSALT and IPSALTS: again,

225 the ERSD was lower for accurate auxiliary data and for the population with spatial trend, and for the  
226 population with lower true population variance.

227 For the 2PS design, there was a large difference in ERSD between the different types of auxiliary data.

228 The best auxiliary data resulted in large improvements of the ERSD relative to the worst auxiliary data.

229 With poor auxiliary data the ERSD was higher than the ERSD of the LPM, and in some cases SI performed

230 almost as well as 2PS. For a different, more even allocation, the ERSD from 2PS was lower, but the

231 accuracy of the auxiliary data still made a difference. The improvement with better auxiliary data was

232 more pronounced in the IPSS and IPSALTS damage population scenarios

233 The Deville estimator ( $\hat{V}_D$ ) for  $\hat{Y}_{LPM}$  overestimated the variance (Table 3). The ratio ( $R$ ) was 1.7-4.7

234 compared to the empirical variance. The Grafström-Schelin variance estimator ( $\hat{V}_{GS}$ ) worked very well in

235 all scenarios and auxiliary data combinations, with a mean estimated variance to empirical variance ratio

236 ( $R$ ) of approximately 1.

237

## 238 Discussion

239 Generally, aerial detection surveys or aerial photo interpretation of damage over affected areas need to  
240 be performed when the damage is visible, but preferably before it has had time to spread further  
241 (Backsen and Howell 2013). This is the case also when other kinds of remote sensing data are used (e.g.  
242 Hall et al. 2016). In forest damage inventories, especially when a new outbreak has been noted and  
243 there is a need to acquire information for decisions on, and support for, potential mitigation strategies,  
244 the time available for setting up the inventory is often limited and the inventory needs to be performed  
245 quickly (e.g. Backsen and Howell 2013). For efficient mitigation of bark beetle outbreaks it is important  
246 to quickly localize affected trees, while the beetles of the next generation are still under the bark of the  
247 recently killed trees (Lindelöw & Schroeder 2008). These trees are often called “green attack trees”, and  
248 are difficult to detect accurately at this stage (Wulder et al 2009). Remotely sensed data about green  
249 attack trees, or data on forest vitality from remote sensing, may not be appropriate for direct  
250 application in mitigation schemes (e.g. Lausch et al. 2013). However, such data may be useful for  
251 efficiently spreading the sample for a forest damage inventory, especially since it is possible to select a  
252 sub-sample from a first-phase sample of auxiliary data (e.g. utilizing high spatial and spectral resolution  
253 data obtained for a sample of the AOI). Since the correlation between this type of data and actual bark  
254 beetle damage may be low, utilization in 2PS sampling may not be efficient due to poor classification  
255 accuracy (Figure 2 and 3). However, the LPM is less sensitive to such problems since the method does  
256 not rely on using the auxiliary information for classification but only for obtaining an efficiently spread  
257 sample in the space of the auxiliary variables. Using the LPM it is possible to utilize other types of  
258 auxiliary data as well, such as map layers with estimated spruce volume, which may be correlated with  
259 spruce bark beetle damage (Kärvemo et al. 2014). Such combinations of auxiliary data contribute to  
260 efficiently spread the sample using LPM and thus result in improved estimates.

261 The spruce bark beetle is one of the most important forest pests in Europe (Schelhaas, Naaburs &  
262 Schuck 2003), and the most important damaging insect on Norway spruce in northern Europe (Weslien  
263 1992). For example, it killed approximately 3 million m<sup>3</sup> of spruce in southern Sweden following two  
264 large storms in 2005-2006, causing additional losses for many forest owners (Långström et al. 2010). In  
265 such a situation it may be important to add as small additional costs as possible to the losses already  
266 incurred, and thus it could be important to keep inventory costs low while still obtaining relevant  
267 information for the mitigation activities (e.g. Herrick 1981).

268 Studying the results obtained from the 2PS design, there was a large difference between the ERSDs from  
269 using different kinds of auxiliary data and, more noticeably, there was a large difference in the ERSD of  
270 the estimator depending on the allocation of the second phase sample. Poor auxiliary data resulted in  
271 higher ERSD, especially for the scenarios where there was a spatial trend in the damage intensity of the  
272 sampled population (i.e. IPSS and IPSALTS). This is interesting since these populations had lower  
273 population variance in comparison to their twin versions. Hence, these results in terms of ERSD were  
274 solely dependent on the spatial difference between the two populations. This volatility was especially  
275 pronounced in scenarios where a large part of S2 was allocated to the stratum with detected damage  
276 trees. However, when the auxiliary information was good and the allocation adequate, 2PS  
277 outperformed LPM in terms of ERSD.

278 While not pursued in this study, the performance of LPM might be improved upon if the auxiliary  
279 information is used for modifying the inclusion probabilities in LPM (e.g. two-phase for stratification  
280 LPM sampling, or by letting the inclusion probabilities be proportional to the numbers of damage trees  
281 in the auxiliary data). In this case it is likely that LPM would have outperformed 2PS with STSI. However,  
282 our application of LPM was straightforward and it is interesting to see how much it improved the  
283 precision of the estimates compared to the SI design.

284 In general, this study resulted in higher ERSDs than those obtained in Roberge et al. (2016), where 2PS  
285 was used as well. However, an important difference is that in the current study we did not assume any  
286 prior knowledge of the domain of interest (i.e. the population susceptible to the damage); in Roberge et  
287 al (2016) such information was available from previously surveyed national forest inventory field plots.  
288 Also, Roberge et al. (2016) showed that wall-to-wall remotely sensed data and post-stratification  
289 improved the precision of estimates further.

290 For variance estimation, two different variance estimators were applied to the LPM-estimator. The  
291 Deville estimator for  $\hat{Y}_{LPM}$  overestimated the variance (table 3), while the Grafström-Schelin variance  
292 estimator worked very well in all scenarios and auxiliary data combinations. The Deville estimator  
293 assumes a high level of randomness in the sample selection and thus worked well for SI samples.  
294 However, it does not exploit the induced stratification effect by the LPM which results in a conservative  
295 variance estimation for such designs. The Grafström-Schelin variance estimator is tailored for well-  
296 spread samples and has previously been shown to sometimes slightly overestimate the variance for  
297 large samples for volume estimates (Grafström and Ringvall, 2013).

298 Results from LPM stand out as consistently better than SI, and relatively unaffected by different kinds of  
299 auxiliary data when compared with the 2PS design. In addition, there is great practical advantage in  
300 avoiding the division into strata and the decision on sample allocation between strata – these issues can  
301 be avoided if the LPM is applied. The two-phase design was used in order to speed up the sample  
302 selection with the LPM algorithm. In this study there was no difference in the precision depending on  
303 the size of the first phase sample. However, it can be noted that large first-phase samples would  
304 increase the cost of LPM and 2PS relative to the cost of SI where only the cost of the field-campaign is  
305 incurred. This way of spreading the sample, applying the LPM in a two-phase strategy, may be indicative  
306 of the competitiveness of LPM in continuous sample selection or for application to larger areas. With

307 this two-phase application it could be used in a continuous approach where unprocessed data from  
308 point clouds (i.e. from ALS or photogrammetric matching of digital aerial images) can be utilized in a first  
309 phase. so while the LPM could utilize the unclassified data space from remotely sensed data together  
310 with other auxiliary GIS-information that may be correlated with the damage event of interest (e.g. GIS  
311 layers of elevation, temperature or precipitation) to select a balanced sample, the 2PS needs processed  
312 data with readily available classifications for the stratification. I.e. the LPM could potentially use data  
313 with less processing to select a sample that is balanced in the auxiliary space, and hence there is less  
314 need for extensive data processing/modeling or classification procedures in order to utilize the  
315 information for designing the inventory than would be the case for applying, for instance, STSI or 2PS  
316 sampling designs. In addition to practicality, auxiliary data spaces from different remote sensing  
317 techniques could be much better than what was examined here, containing more information than the  
318 classified data we used in this study. If for instance the variable to estimate had been the damaged  
319 volume, first return data or highest point-cloud information would have been correlated with the  
320 volume, thus further improving the LPM's performance.

321 Overall, 2PS sampling is a competitive and efficient means of utilizing auxiliary information in selection.  
322 With good auxiliary information, it is possible to choose a good allocation and sample 2PS with good  
323 results, but this may be difficult when the information is flawed, and its true state is unknown.

324 For variance estimation it is advisable to utilize the  $\hat{V}_{GS}$  estimator (eq. 5).

325 In conclusion the LPM has been shown to be a better choice than SI in all cases evaluated. Considering  
326 that more auxiliary data sources could potentially be utilized, LPM stands out as a straightforward  
327 approach to use such data to improve forest damage inventories.

## 328 Acknowledgements

329 We wish to thank two anonymous reviewers for their valuable comments that helped us to improve the  
330 manuscript. We also wish to thank Sören Wulff and the staff of the Swedish NFI and TFDI for their  
331 valuable work contributing to building the simulated populations. Cornelia Roberge was supported by  
332 grant 2008-546 from the Swedish Research Council Formas to Anna Hedström-Ringvall.

## 333 References

- 334 Allen, C. D., et al. 2010. A global overview of drought and heat-induced tree mortality reveals emerging  
335 climate change risks for forests. *Forest Ecology and Management* 259(4): 660-684.  
336
- 337 Aamlid, D., et al. 2000. Changes of forest health in Norwegian boreal forests during 15 years. *Forest*  
338 *Ecology and Management* 127(1-3): 103-118.  
339
- 340 Backsen, J. C. and Howell, B. 2013. Comparing aerial detection and photo interpretation for conducting  
341 forest health surveys. *Western Journal of Applied Forestry* 28(1): 3-8.  
342
- 343 Bennett, D. D. and Tkacz, B. M. 2008. Forest health monitoring in the United States: a program overview.  
344 *Australian Forestry*. 71(3): 223-228.  
345
- 346 Bivand, R., Keitt, T. and Rowlingson B. 2016. rgdal: Bindings for the Geospatial Data Abstraction Library.  
347 R package version 1.1-10. <https://CRAN.R-project.org/package=rgdal>  
348
- 349 Carnegie, A. J. 2008. A decade of forest health surveillance in Australia: an overview. *Australian Forestry*.  
350 71(3): 161-163.

- 351
- 352 Ciesla, W.M. 2000. Remote sensing in forest health protection (FHTET Report No. 00-03). Retrieved from  
353 [www.fs.fed.us/foresthealth/technology/pdfs/RemoteSensingForestHealth00\\_03.pdf](http://www.fs.fed.us/foresthealth/technology/pdfs/RemoteSensingForestHealth00_03.pdf)  
354 (13:17,2016-09-06)
- 355
- 356 Corbett, L. J., Withey, P., Lantz, V. A., & Ochuodho T. O. 2015. The economic impact of the mountain  
357 pine beetle infestation in British Columbia: provincial estimates from a CGE analysis. *Forestry*.  
358 doi: 10.1093/forestry/cpv042
- 359
- 360 Dale, V. H., Joyce, L. A., McNulty, S., Neilson, R. P., Ayres, M. P., Flannigan, M. D., et al. 2001. Climate  
361 Change and Forest Disturbances: Climate change can affect forests by altering the frequency,  
362 intensity, duration, and timing of fire, drought, introduced species, insect and pathogen  
363 outbreaks, hurricanes, windstorms, ice storms, or landslides. *BioScience*, 51(9), 723-734,  
364 doi:10.1641/0006-3568(2001)051[0723:ccafd]2.0.co;2.
- 365
- 366 Deville, J. C. 1993. Estimation de la variance pour les enquêtes en deux phases. Manuscript. Paris,  
367 France: INSEE.
- 368
- 369 Dowle, M., Srinivasan, A., Short, T., Lianoglou S., with contributions from Saporta, R., and Antonyan, E.  
370 2015. data.table: Extension of Data.frame. R package version 1.9.6. [https://CRAN.R-](https://CRAN.R-project.org/package=data.table)  
371 [project.org/package=data.table](https://CRAN.R-project.org/package=data.table)
- 372

- 373 Ferretti, M., König, N., Rautio, P., & Sase, H. 2009. Quality assurance (QA) in international forest  
374 monitoring programmes: activity, problems and perspectives from East Asia and Europe. *Annals*  
375 *of Forest Science*, 66(4), 1-12.
- 376
- 377 Grafström, A. and Lisic, J. 2016. *BalancedSampling: Balanced and Spatially Balanced Sampling*. R package  
378 version 1.5.2. <https://CRAN.R-project.org/package=BalancedSampling>
- 379
- 380 Grafström, A., and Lundström, N.L.P. 2013. Why well spread probability samples are balanced. *Open*  
381 *Journal of Statistics*, 3(1): 36-41. doi:10.4236/ojs.2013.31005.
- 382
- 383 Grafström, A., and Ringvall, A.H. 2013. Improving forest field inventories by using remote sensing data in  
384 novel sampling designs. *Can. J. For. Res.* 43(11):1015-1022. doi: 10.1139/cjfr-2013-0123.
- 385
- 386 Grafström, A., and Schelin, L. 2013. How to select representative samples. *Scand.J. Stat.* 41(2): 277-290.  
387 doi: 10.1111/sjos.12016.
- 388
- 389 Grafström, A., Lundström, N.L.P., and Schelin, L. 2012. Spatially balanced sampling through the Pivotal  
390 method. *Biometrics*, 68(2): 514-520. doi: 10.1111/j.1541-0420.2011.01699.x.
- 391
- 392 Grafström, A., Saarela, S., & Ene, L. T. 2014. Efficient sampling strategies for forest inventories by  
393 spreading the sample in auxiliary space. *Canadian Journal of Forest Research*, 44(10), 1156-  
394 1164.
- 395

- 396 Hall, R. J., et al. 2016. Remote sensing of forest pest damage: a review and lessons learned from a  
397 Canadian perspective\*. *The Canadian Entomologist*: 1-61.  
398
- 399 Hais, M., et al. 2009. Comparison of two types of forest disturbance using multitemporal Landsat  
400 TM/ETM+ imagery and field vegetation data. *Remote Sensing of Environment* 113(4): 835-845.  
401
- 402 Herrick, O. W. (1981). Forest Pest Management Economics--Application to the Gypsy Moth. *Forest*  
403 *Science*, 27(1), 128-138.  
404
- 405 Hijmans, Robert J. (2016). raster: Geographic Data Analysis and Modeling. R package version 2.5-8.  
406 <https://CRAN.R-project.org/package=raster>  
407
- 408 Kärvmö, S., Van Boeckel, T. P., Gilbert, M., Grégoire, J.-C. & Schroeder, M. (2014). Large-scale risk  
409 mapping of an eruptive bark beetle – Importance of forest susceptibility and beetle pressure.  
410 *Forest Ecology and Management*. 318:158-166.  
411
- 412 Långström, B., Lindelöw, Å., Schroeder, M., Björklund, N. & Öhrn, P. (2010). The spruce bark beetle  
413 outbreak in Sweden following the January-storms in 2005 and 2007. Available from:  
414 [http://pub.epsilon.slu.se/5076/1/langstrom\\_b\\_etal\\_100823.pdf](http://pub.epsilon.slu.se/5076/1/langstrom_b_etal_100823.pdf). [2016-10-20]  
415
- 416 Lausch, A., Heurich, M., Gordalla, D., Dobner, H.-J., Gwilym-Margianto, S. and Salbach, C. (2013).  
417 Forecasting potential bark beetle outbreaks based on spruce forest vitality using hyperspectral  
418 remote-sensing techniques at different scales. *Forest Ecology and Management* 308:76-89.  
419

- 420 Lindelöw, Å. & Schroeder, M. (2008). The storm "Gudrun" and the spruce bark beetle in Sweden. In:  
421 Steyrer, G., et al. (Eds.) Second meeting of Forest Protection and Forest Phytosanitary  
422 Specialists, Vienna, Austria, 27-28 November 2007. Forstschutz aktuell nr 44, Bundesforschungs-  
423 und Ausbildungszentrum für wald, Naturgefahren und Landschaft (BFW), Vienna, Austria.  
424
- 425 Mery, G., Alfaro, R.I., Kanninen, M., and Lobovikov, M. 2005. Forests in the global balance —changing  
426 paradigms. IUFRO World Series, Volume 17. International Union of Forestry Research  
427 Organizations (IUFRO), Vienna, Austria. Retrieved from:  
428 <http://www.iufro.org/science/special/wfse/forests-society-global-drivers/> (2016-09-07 at 04:57)  
429
- 430 Näsi, R., et al. (2015). Using UAV-Based Photogrammetry and Hyperspectral Imaging for Mapping Bark  
431 Beetle Damage at Tree-Level. *Remote Sensing* 7(11): 15467-15493.  
432
- 433 Ortiz, S.M., Breidenbach, J., Kändler, G. 2013. Early Detection of Bark Beetle Green Attack Using  
434 TerraSAR-X and RapidEye Data. *Remote Sens.* 2013, 5, 1912-1931.  
435
- 436 Perpinan Lamigueiro, O., and Hijmans, R., 2016, meteoForecast. R package version 0.40.  
437
- 438 R Core Team (2016). R: A language and environment for statistical computing. R Foundation for  
439 Statistical Computing, Vienna, Austria. URL <https://www.R-project.org/>.  
440
- 441 Reese, H., Nilsson, M., Granqvist-Pahlén, T., Hagner, O., Joyce, S., Tingelöf, U., et al. 2003. Countrywide  
442 Estimates of Forest Variables Using Satellite Data and Field Data from the National Forest  
443 Inventory. *AMBIO: A Journal of the Human Environment*, 32(8), 542-548.

- 444
- 445 Roberge, C., Wulff, S., Reese, H., & Ståhl, G. 2016. Improving the precision of sample-based forest  
446 damage inventories through two-phase sampling and post-stratification using remotely sensed  
447 auxiliary information. *Environmental Monitoring and Assessment*, 188(4), 1-21. doi:  
448 10.1007/s10661-016-5208-4
- 449
- 450 Rullan-Silva, C. D., Olthoff, A. E., Delgado de la Mata, J. A. & Pajares-Alonso J. A. (2013). Remote  
451 monitoring of forest insect defoliation. A review. *Forest Systems* 2013 22(3): 377-391
- 452
- 453 Schelhaas, M.-J., Nabuurs, G.-J. & Schuck, A. (2003) Natural disturbances in the European forests in the  
454 19th and 20th centuries. *Global change biology*, 9: 1620–1633. doi:10.1046/j.1365-  
455 2486.2003.00684.x
- 456
- 457 Solberg, S. 2010. Mapping gap fraction, LAI and defoliation using various ALS penetration variables.  
458 *International Journal of Remote Sensing* 31(5): 1227-1244.
- 459
- 460 Särndal, C.-E., Swensson, B., & Wretman, J. H. 1992. Model assisted survey sampling. New York:  
461 Springer-Verlag.
- 462
- 463 Tillé, Y., and Matei, A. 2015. *sampling: Survey Sampling*. R package version 2.7.  
464 <https://CRAN.R-project.org/package=sampling>
- 465
- 466 Trumbore, S., Brando, P. and Hartmann, H. (2015) Forest health and global change. *Science*.  
467 349(6250):814-818.

468

469 Weslien, J. (1992), Monitoring *Ips typographus* (L.) populations and forecasting damage<sup>1</sup>. Journal of  
470 Applied Entomology, 114: 338–340. doi:10.1111/j.1439-0418.1992.tb01136.x

471

472 Wickham, H. 2009. ggplot2: Elegant Graphics for Data Analysis. Springer-Verlag, New York, 2009.

473

474 Wulder, M.A., White, J.C., Carroll, A.L. and Coops N.C. (2009). Challenges for the operational detection  
475 of mountain pine beetle green attack with remote sensing. The Forestry Chronicle 85(1):32-38.

476

477 Wulff, S., Lindelöw, Å., Lundin, L., Hansson, P., Axelsson, A.-L., Barklund, P., Wijk, S., Ståhl, G. 2012.

478 Adapting forest health assessments to changing perspectives on threats—a case example from  
479 Sweden. Environmental Monitoring and Assessment, 184(4), 2453-2464. doi: 10.1007/s10661-  
480 011-2130-7

481

482 **Table 1.** Number of damage trees ( $y$ ) and affected grid-cells ( $1/0$ ) in the simulated populations.

	IPS		IPSS		IPSALT		IPSALTS	
	1/0	$y$	1/0	$y$	1/0	$y$	1/0	$y$
<b>True Total</b>	$282 \times 10^3$	$846 \times 10^3$	$282 \times 10^3$	$662 \times 10^3$	$167 \times 10^3$	$502 \times 10^3$	$171 \times 10^3$	$396 \times 10^3$
<b>Mean</b>	0.20	0.59	0.20	0.46	0.12	0.35	0.12	0.27
<b><math>\sigma</math></b>	0.40	1.34	0.40	1.05	0.32	1.07	0.32	0.83
<b>Maximum</b>	1	12	1	10	1	12	1	10
<b>Minimum</b>	0	0	0	0	0	0	0	0

483

484

Draft

485 **Table 2.** Empirical relative standard deviations in % over 1 000 repetitions.

Population	Aux.data	Design	$n_1 = 3\ 600$				$n_1 = 10\ 000$			
			$n_2=50$	$n_2=100$	$n_2=150$	$n_2=200$	$n_2=50$	$n_2=100$	$n_2=150$	$n_2=200$
IPS	DTC60H	LPM	22	16	13	12	23	16	13	11
		2PS_40	21	15	12	10	22	15	12	11
		2PS_20	25	19	16	13	25	19	15	13
	DTC60L	LPM	20	14	11	10	20	14	11	<b>10</b>
		2PS_40	20	13	11	<b>10</b>	20	13	11	10
		2PS_20	26	18	15	13	25	17	14	13
	DTC90H	LPM	20	14	12	<b>10</b>	21	14	11	10
		2PS_40	15	10	<b>9</b>	<b>7</b>	15	11	<b>9</b>	<b>7</b>
		2PS_20	15	11	<b>9</b>	<b>8</b>	15	10	<b>8</b>	<b>7</b>
	DTC90L	LPM	18	12	10	<b>9</b>	18	12	<b>10</b>	<b>8</b>
		2PS_40	11	<b>8</b>	<b>7</b>	<b>6</b>	11	<b>8</b>	<b>6</b>	<b>6</b>
		2PS_20	11	<b>9</b>	<b>7</b>	<b>6</b>	12	<b>9</b>	<b>7</b>	<b>6</b>
IPSS	DTC60H	LPM	23	17	14	12	23	16	14	12
		2PS_40	22	16	13	11	22	15	13	11
		2PS_20	31	21	18	14	29	21	16	14
	DTC60L	LPM	20	13	11	<b>10</b>	19	13	11	<b>9</b>
		2PS_40	21	15	12	11	21	15	12	11
		2PS_20	30	21	16	15	29	19	17	14
	DTC90H	LPM	20	14	11	<b>10</b>	21	14	11	<b>10</b>
		2PS_40	15	11	<b>9</b>	<b>8</b>	16	11	<b>9</b>	<b>8</b>
		2PS_20	16	11	<b>9</b>	<b>8</b>	16	11	<b>9</b>	<b>8</b>
	DTC90L	LPM	17	11	<b>9</b>	<b>8</b>	17	11	<b>9</b>	<b>8</b>
		2PS_40	12	<b>8</b>	<b>7</b>	<b>6</b>	11	<b>8</b>	<b>6</b>	<b>6</b>
		2PS_20	13	<b>9</b>	<b>8</b>	<b>7</b>	12	<b>9</b>	<b>8</b>	<b>7</b>
IPSALT	DTC60H	LPM	32	23	19	16	33	23	18	16
		2PS_40	30	21	16	14	29	20	17	14
		2PS_20	37	23	20	18	34	25	20	17
	DTC60L	LPM	26	18	15	13	28	18	15	13
		2PS_40	25	18	15	13	25	17	15	13
		2PS_20	33	24	20	17	33	25	20	17
	DTC90H	LPM	28	20	16	14	28	19	15	14
		2PS_40	19	14	12	<b>10</b>	19	14	11	<b>10</b>
		2PS_20	19	14	11	10	20	14	11	<b>10</b>
	DTC90L	LPM	24	17	14	12	24	16	13	11
		2PS_40	13	11	<b>9</b>	<b>8</b>	12	<b>9</b>	<b>8</b>	<b>6</b>
		2PS_20	15	11	10	<b>9</b>	15	10	<b>8</b>	<b>8</b>
IPSALTS	DTC60H	LPM	33	22	19	16	33	23	19	16
		2PS_40	30	20	18	16	33	22	18	15
		2PS_20	39	27	23	20	41	26	22	20
	DTC60L	LPM	26	19	15	13	26	17	15	12
		2PS_40	28	21	16	14	30	19	18	14
		2PS_20	42	28	24	19	39	28	23	19
	DTC90H	LPM	28	20	16	14	27	20	16	14
		2PS_40	20	15	12	10	20	14	11	<b>10</b>
		2PS_20	20	16	13	10	21	14	11	10
	DTC90L	LPM	23	15	12	10	22	15	12	<b>10</b>
		2PS_40	13	<b>10</b>	<b>9</b>	<b>8</b>	14	<b>9</b>	<b>7</b>	<b>7</b>
		2PS_20	19	12	11	<b>10</b>	16	11	11	<b>8</b>

486 **Note:** ERSD below 10% are in bold text and above 25% are cursive.

487 **Table 3.** Ratio of mean  $\hat{V}_{GS}(\hat{Y}_{LPM})$  and mean  $\hat{V}_D(\hat{Y}_{LPM})$  to empirical variance over 1 000 repetitions.

Population	Aux.data		$n_1 = 3\ 600$				$n_1 = 10\ 000$			
			$n_2=50$	$n_2=100$	$n_2=150$	$n_2=200$	$n_2=50$	$n_2=100$	$n_2=150$	$n_2=200$
IPS	DTC60H	$\hat{V}_{GS}$	1.1	1.0	1.0	0.9	1.0	0.9	1.0	1.0
		$\hat{V}_D$	<b>2.1</b>	<b>2.1</b>	<b>2.1</b>	<b>1.9</b>	<b>1.9</b>	<b>1.9</b>	<b>2.0</b>	<b>2.1</b>
	DTC60L	$\hat{V}_{GS}$	1.0	1.0	1.0	0.9	1.1	1.0	1.0	0.9
		$\hat{V}_D$	<b>2.5</b>	<b>2.7</b>	<b>2.8</b>	<b>2.6</b>	<b>2.6</b>	<b>2.7</b>	<b>2.9</b>	<b>2.8</b>
	DTC90H	$\hat{V}_{GS}$	0.9	1.0	0.9	1.0	0.8	0.9	1.0	0.9
		$\hat{V}_D$	<b>2.6</b>	<b>2.9</b>	<b>2.6</b>	<b>2.7</b>	<b>2.5</b>	<b>2.7</b>	<b>2.8</b>	<b>2.5</b>
	DTC90L	$\hat{V}_{GS}$	1.0	1.0	1.0	1.0	1.0	1.1	1.0	1.1
		$\hat{V}_D$	<b>3.3</b>	<b>3.5</b>	<b>3.3</b>	<b>3.6</b>	<b>3.2</b>	<b>3.7</b>	<b>3.6</b>	<b>4.1</b>
IPSSS	DTC60H	$\hat{V}_{GS}$	1.0	1.0	1.0	0.9	1.1	1.0	1.0	0.9
		$\hat{V}_D$	<b>1.9</b>	<b>1.8</b>	<b>1.9</b>	<b>1.8</b>	<b>1.9</b>	<b>1.9</b>	<b>1.9</b>	<b>1.8</b>
	DTC60L	$\hat{V}_{GS}$	1.1	1.0	0.9	0.9	1.1	1.1	1.0	1.0
		$\hat{V}_D$	<b>2.8</b>	<b>2.9</b>	<b>2.7</b>	<b>2.7</b>	<b>2.8</b>	<b>2.9</b>	<b>2.7</b>	<b>2.9</b>
	DTC90H	$\hat{V}_{GS}$	1.0	0.9	1.0	1.0	0.9	1.0	1.0	1.0
		$\hat{V}_D$	<b>2.6</b>	<b>2.6</b>	<b>2.7</b>	<b>2.8</b>	<b>2.5</b>	<b>2.7</b>	<b>2.9</b>	<b>2.7</b>
	DTC90L	$\hat{V}_{GS}$	1.1	1.1	1.0	0.9	1.2	1.1	1.0	1.0
		$\hat{V}_D$	<b>3.5</b>	<b>4.2</b>	<b>4.1</b>	<b>4.1</b>	<b>3.8</b>	<b>4.1</b>	<b>4.3</b>	<b>4.4</b>
IPSALT	DTC60H	$\hat{V}_{GS}$	1.0	0.9	0.9	1.0	1.0	0.9	1.0	1.0
		$\hat{V}_D$	<b>1.9</b>	<b>1.8</b>	<b>1.8</b>	<b>1.9</b>	<b>1.8</b>	<b>1.7</b>	<b>1.9</b>	<b>1.9</b>
	DTC60L	$\hat{V}_{GS}$	1.1	1.0	1.0	0.9	1.0	1.1	0.9	0.9
		$\hat{V}_D$	<b>2.9</b>	<b>2.8</b>	<b>2.8</b>	<b>2.9</b>	<b>2.5</b>	<b>3.0</b>	<b>2.8</b>	<b>2.9</b>
	DTC90H	$\hat{V}_{GS}$	0.9	0.9	0.9	0.9	0.9	1.0	1.0	0.9
		$\hat{V}_D$	<b>2.5</b>	<b>2.5</b>	<b>2.5</b>	<b>2.4</b>	<b>2.5</b>	<b>2.6</b>	<b>2.7</b>	<b>2.5</b>
	DTC90L	$\hat{V}_{GS}$	1.0	0.9	0.9	0.9	1.0	1.1	1.0	1.0
		$\hat{V}_D$	<b>3.4</b>	<b>3.2</b>	<b>3.3</b>	<b>3.5</b>	<b>3.3</b>	<b>3.7</b>	<b>3.8</b>	<b>3.9</b>
IPSALTS	DTC60H	$\hat{V}_{GS}$	1.0	1.0	1.0	1.0	1.0	1.0	1.0	1.1
		$\hat{V}_D$	<b>1.7</b>	<b>1.8</b>	<b>1.7</b>	<b>1.7</b>	<b>1.7</b>	<b>1.7</b>	<b>1.7</b>	<b>1.9</b>
	DTC60L	$\hat{V}_{GS}$	1.1	0.9	0.9	0.9	<b>1.2</b>	1.1	1.0	1.0
		$\hat{V}_D$	<b>2.7</b>	<b>2.5</b>	<b>2.5</b>	<b>2.7</b>	<b>2.9</b>	<b>3.1</b>	<b>2.9</b>	<b>3.0</b>
	DTC90H	$\hat{V}_{GS}$	0.9	1.0	1.0	0.9	1.1	1.0	1.0	1.0
		$\hat{V}_D$	<b>2.3</b>	<b>2.4</b>	<b>2.4</b>	<b>2.3</b>	<b>2.6</b>	<b>2.4</b>	<b>2.5</b>	<b>2.5</b>
	DTC90L	$\hat{V}_{GS}$	1.0	1.0	1.0	1.0	1.1	1.1	1.0	1.1
		$\hat{V}_D$	<b>3.6</b>	<b>4.0</b>	<b>4.2</b>	<b>4.3</b>	<b>3.9</b>	<b>4.3</b>	<b>4.5</b>	<b>4.7</b>

488 **Note:**  $\hat{R} < 0.8$  and  $\hat{R} < 1.2$  are marked in bold font.

489

490 **Figure 1.** 900 km<sup>2</sup> landscape with simulated true numbers of damage trees for the four damage  
491 populations **a.** IPS, **b.** IPSS, **c.** IPSALT, **d.** IPSALTS and **e.** true spruce volume layer from which damage  
492 were simulated.

493

494 **Figure 2.** ERSD for  $n_1=10\ 000$  and all combinations of damage, sample size, sampling strategy and  
495 auxiliary information used. ERSD for SI is included as a straight line.

496

497 **Figure 3.** ERSD for  $n_1=3\ 600$ , and all combinations of damage, sample size, sampling strategy and  
498 auxiliary information used. ERSD from SI design in straight line across.

499

Draft

500 **Appendices**

501

502 **Table A1.** ERSD of SI for each damage scenario and sample size.

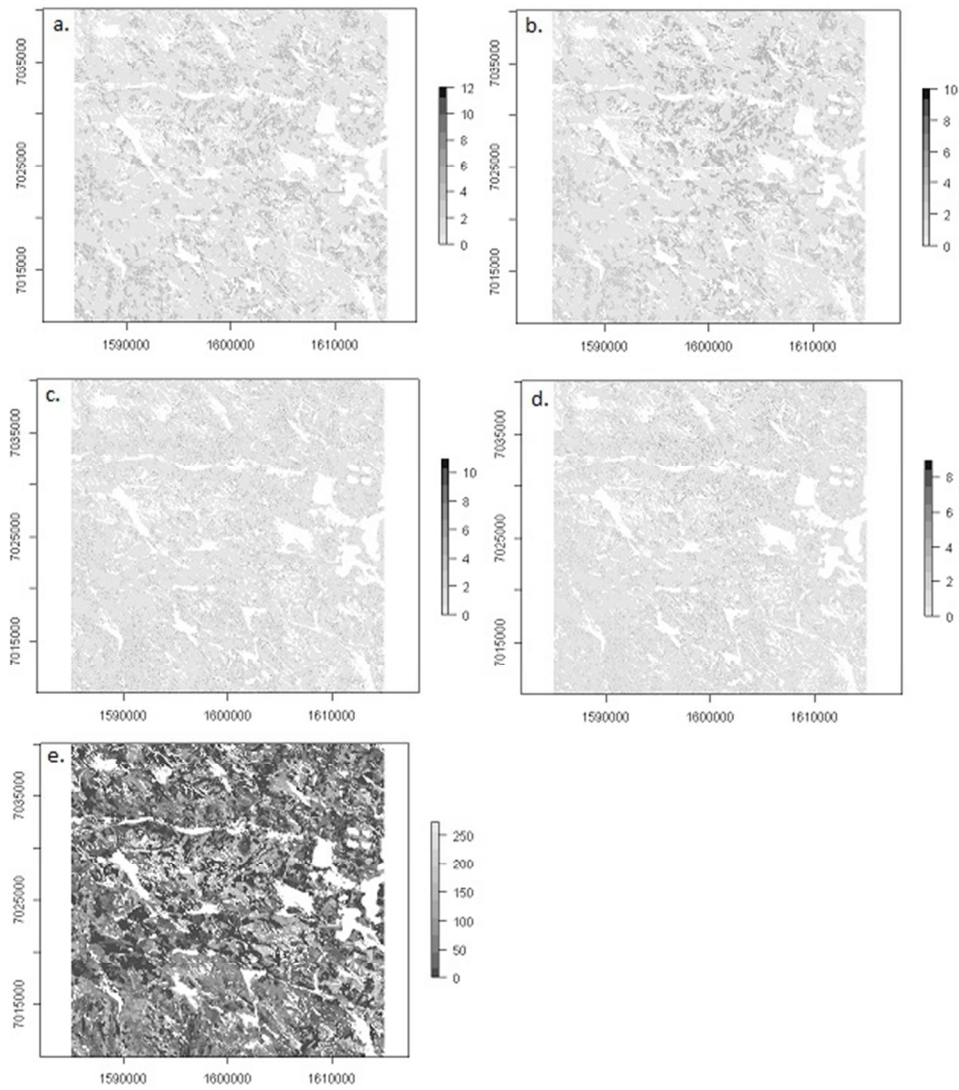
	Sample size	50	100	150	200
Damage	IPS	32%	23%	18%	16%
	IPSALT	45%	30%	24%	21%
	IPSALTS	43%	29%	25%	22%
	IPSS	33%	23%	18%	16%

Draft

**Table A2.** Actual sensitivity of simulated auxiliary spaces – True positive rates (ie. DTC 1-1,2-2,3-3 etc, but for D: 1-1/0-0))

<b>Damage Population</b>	<b>Auxiliary data</b>	<b>Sensitivity (exact DTC)</b>	<b>Sensitivity (D)</b>
IPS	DTC90L	0.925	0.983
IPS	DTC90H	0.925	0.983
IPS	DTC60L	0.604	0.880
IPS	DTC60H	0.604	0.880
IPSS	DTC90L	0.919	0.974
IPSS	DTC90H	0.920	0.975
IPSS	DTC60L	0.582	0.828
IPSS	DTC60H	0.583	0.830
IPSALT	DTC90L	0.925	0.983
IPSALT	DTC90H	0.925	0.983
IPSALT	DTC60L	0.607	0.881
IPSALT	DTC60H	0.603	0.879
IPSALTS	DTC90L	0.923	0.975
IPSALTS	DTC90H	0.923	0.975
IPSALTS	DTC60L	0.590	0.830
IPSALTS	DTC60H	0.586	0.829

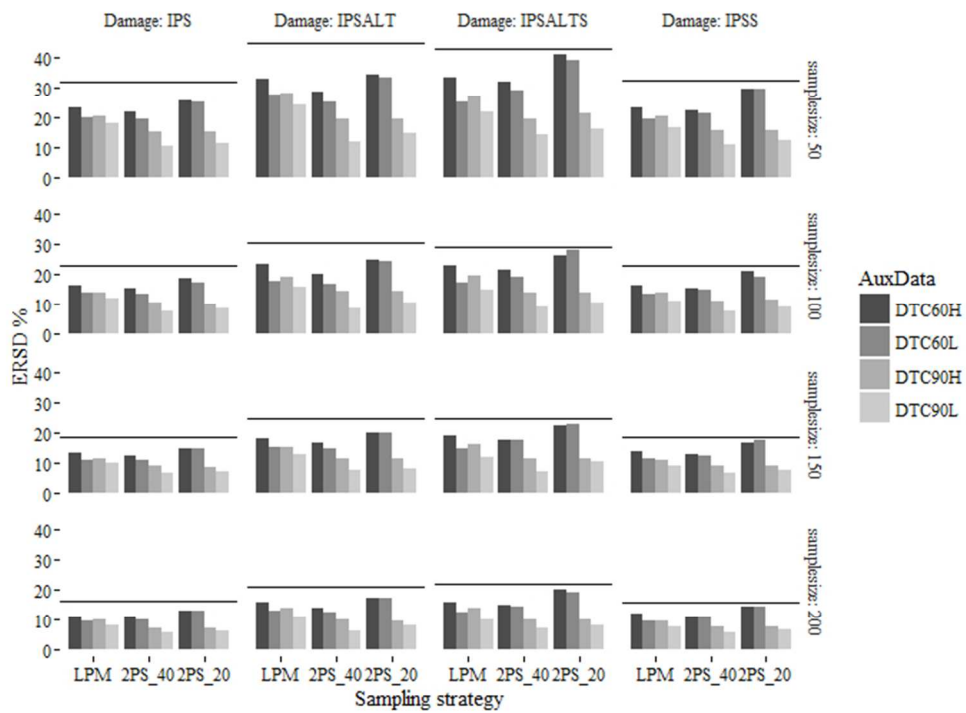
Draft



900 km<sup>2</sup> landscape with simulated true numbers of damage trees for the four damage populations a. IPS, b. IPSS, c. IPSALT, d. IPSALTS and e. true spruce volume layer from which damage were simulated.

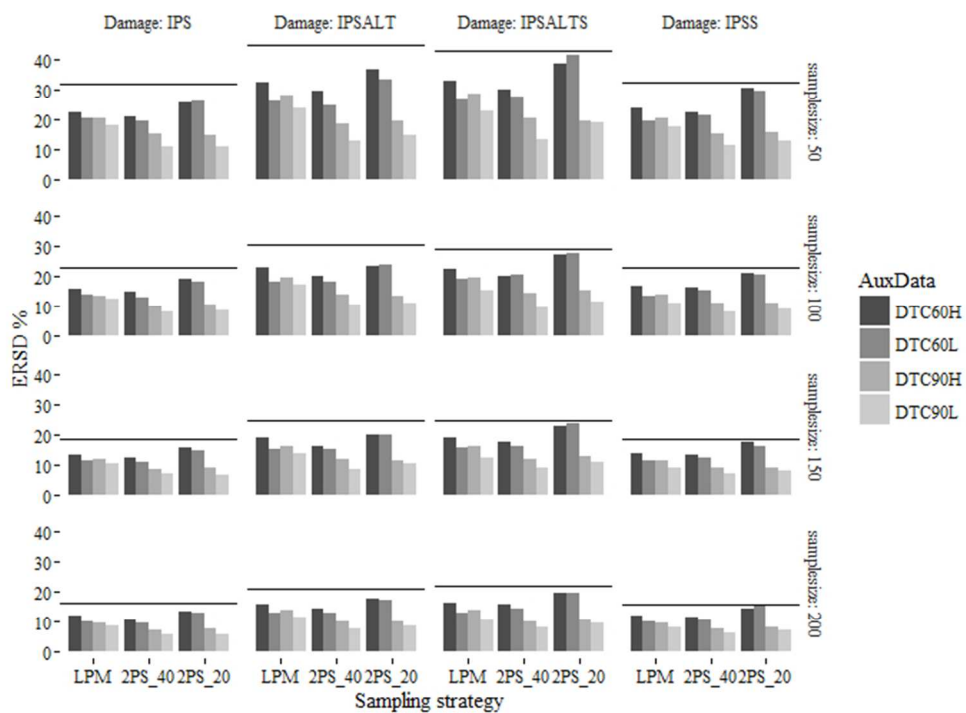
Figure 1

174x207mm (96 x 96 DPI)



ERSD for  $n_1=10\ 000$  and all combinations of damage, sample size, sampling strategy and auxiliary information used. ERSD for SI is included as a straight line.

Figure 2



ERSD for  $n_1=3600$ , and all combinations of damage, sample size, sampling strategy and auxiliary information used. ERSD from SI design in straight line across.

Figure 3